Glucose Oxidase Catalyzed Self-Assembly of Bioelectroactive Gold Nanostructures

Heather R. Luckarift,[a,b]* *Dmitri Ivnitski*,[c] *Rosalba Rincón*,[c] *Plamen Atanassov*,[c]* *Glenn R. Johnson*[a]

[a] Microbiology and Applied Biochemistry (AFRL/RXQL), Air Force Research Laboratory, 139 Barnes Drive, Suite #2, Tyndall Air Force Base, FL 32403, USA
*e-mail: heather.luckarift.ctr@tyndall.af.mil; plamen@unm.edu
[b] Universal Technology Corporation, 1270 N. Fairfield Road, Dayton, OH 45432, USA
[c] Chemical and Nuclear Engineering Department, University of New Mexico, Albuquerque, NM 87131, USA

Received: June 15, 2009
Accepted: October 1, 2009

Abstract
Glucose oxidase catalyzes the formation of metallic gold particles in immediate proximity of the protein from gold (III) chloride in the absence of any other catalytic or reductive substrates. The protein-mediated gold reduction reaction leads to size-controllable gold particle formation and concomitant association of the enzyme in an electrically conductive metallic template. Such an enzyme immobilization strategy provides a simple and rapid method to create an intimate interface between glucose oxidase and a conductive matrix, which can be joined to an electrode surface. Model electrodes were prepared by entraining the glucose oxidase/gold particles onto carbon paper. Voltammetry of the resulting electrodes revealed stable oxidation and reduction peaks at a potential close to that of the standard value for the FAD/$FADH_2$ cofactor of immobilized glucose oxidase. The gold electrodes exhibit catalytic activity in the presence of glucose confirming the entrapment of active glucose oxidase within the gold architecture. The resulting composite material can be successfully integrated with electrodes of various designs for biosensor and biofuel cell applications.

Keywords: Gold reduction, Glucose oxidase, Electron transfer, Nanocomposites, Self-assembly

DOI: 10.1002/elan.200980003

1. Introduction

The ability to create stable enzyme/metal nanocomposites that retain enzyme activity at high surface-to-volume ratios provides excellent opportunities in catalysis, biosensing and biofuel cell applications [1–4]. The synthesis of gold nanoparticles with controllable shapes and structural properties, in particular, has provided significant advances in glucose sensing due to unique optical and electronic properties [5, 6]. Gold nanoparticles with the appropriate dimensions can also act as a bridge between the redox center of an enzyme and the bulk electrode material to facilitate direct electron transfer (DET) [2, 3, 6]. DET is advantageous as it negates the use of mediators and electron transfer occurs at a potential close to the redox potential of the enzyme itself [7, 8]. In the absence of a suitable "connection" (electrochemical mediator, charge transfer relay, conductive polymer matrix), however, electrons generated at the FAD/$FADH_2$ active site of glucose oxidase (GOx) must tunnel ca. 15 Å through the protein shell, severely limiting DET efficiency [9]. Attempts have been made to reduce the electron tunneling distance by using conductive nanostructures to shuttle electrons [10]. Manipulations of such nanoparticles, however, have proven extremely time sensitive and their practical use depends strongly upon the protocols applied. Carbon nanotubes (CNT) for example provide an excellent conduit for electrical communication and electron transfer rates of ca. 1–3 s^{-1} have been reported for immobilized GOx [7, 11, 12]. Creating architectures containing CNT, however, has proven difficult and integration of enzymes with CNT and with the electrode interface continues to present challenges for scale-up and manufacturability. Similarly, gold nanoparticles, structured on the electrode interface can act as a scaffold for GOx immobilization and mediate DET [6, 13, 14]. In the presence of gold nanoparticles of specific size, the electron transfer distance is significantly decreased, leading to an increase in the electron tunneling rate of more than 1000-fold in some cases [15]. Therefore, there is considerable interest in methods for controlling the preparation of well-defined gold nanoparticles of different size and shape. It is ever more important to have those methods involve simultaneous enzyme immobilization with a conductive phase, preferably forming in a controlled synergistic fashion.

A wealth of chemical approaches have been developed for the synthesis of gold nanoparticles including the process reduction of metal salts by reagents such as sodium borohydride, hydroxylamine and polyvinyl pyrrolidone [1–3, 16]. While chemical methods for gold reduction are well documented, many biological materials including plant extracts, bacterial and fungal strains will catalyze the reduction of gold salts to gold nanoparticles of differing size and morphologies [16–21]. As such, the interaction of biomolecules with colloidal gold as well as the study of enzymatic activity of bioconjugates has also attracted attention [22–25].

WILEY InterScience DISCOVER SOMETHING GREAT
© 2010 Wiley-VCH Verlag GmbH & Co. KGaA, Weinheim

Report Documentation Page

Form Approved
OMB No. 0704-0188

Public reporting burden for the collection of information is estimated to average 1 hour per response, including the time for reviewing instructions, searching existing data sources, gathering and maintaining the data needed, and completing and reviewing the collection of information. Send comments regarding this burden estimate or any other aspect of this collection of information, including suggestions for reducing this burden, to Washington Headquarters Services, Directorate for Information Operations and Reports, 1215 Jefferson Davis Highway, Suite 1204, Arlington VA 22202-4302. Respondents should be aware that notwithstanding any other provision of law, no person shall be subject to a penalty for failing to comply with a collection of information if it does not display a currently valid OMB control number.

1. REPORT DATE	2. REPORT TYPE	3. DATES COVERED
2009		**00-00-2009 to 00-00-2009**

4. TITLE AND SUBTITLE	5a. CONTRACT NUMBER
Glucose Oxidase Catalyzed Self-Assembly of Bioelectroactive Gold Nanostructures	5b. GRANT NUMBER
	5c. PROGRAM ELEMENT NUMBER
6. AUTHOR(S)	5d. PROJECT NUMBER
	5e. TASK NUMBER
	5f. WORK UNIT NUMBER
7. PERFORMING ORGANIZATION NAME(S) AND ADDRESS(ES) **Microbiology and Applied Biochemistry (AFRL/RXQL), Air Force Research Laboratory,139 Barnes Drive, Suite #2,Tyndall Air Force Base,FL,32403**	8. PERFORMING ORGANIZATION REPORT NUMBER
9. SPONSORING/MONITORING AGENCY NAME(S) AND ADDRESS(ES)	10. SPONSOR/MONITOR'S ACRONYM(S)
	11. SPONSOR/MONITOR'S REPORT NUMBER(S)

12. DISTRIBUTION/AVAILABILITY STATEMENT
Approved for public release; distribution unlimited

13. SUPPLEMENTARY NOTES
Electroanalysis 2010, 22, No. 7-8, 784 - 792

14. ABSTRACT

15. SUBJECT TERMS

16. SECURITY CLASSIFICATION OF:			17. LIMITATION OF ABSTRACT	18. NUMBER OF PAGES	19a. NAME OF RESPONSIBLE PERSON
a. REPORT **unclassified**	b. ABSTRACT **unclassified**	c. THIS PAGE **unclassified**	**Same as Report (SAR)**	**10**	

GOx is known to catalyze gold reduction but only in the presence of glucose, due to the catalytic formation of H_2O_2 that in turn acts as a reducing agent for gold [10, 13, 26]. We report herein that GOx catalyzes the reduction of Au^{3+} to metallic Au in the form of particles whose size depends on the kinetics of the nucleation process. This process occurs in the absence of glucose or peroxide, formed as a result of enzymatic oxidation of glucose or any other reducing agent. The enzyme also acts as a self-assembly factor in the formation of gold particles and ultimately becomes entrained within the resulting gold nanostructures. The resulting glucose oxidase/gold (GOx-Au) composites demonstrate DET between the FAD/$FADH_2$ redox center of GOx and the gold particles. To our knowledge, the reduction of $AuCl_4^-$ by a redox-active enzyme that in turn retains its catalytic activity in the resulting gold particle has not been reported previously. The direct encapsulation of enzymes within gold provides an opportunity to develop redox-active conductive material for application in the development of micro-sized enzyme-based fuel cells and label-free biosensing systems.

2. Experimental

2.1. Materials

Type II-S GOx from *Aspergillus niger* (EC 1.1.3.4) and gold (III) chloride solution (ca. 30 wt% in dilute HCl) were obtained from Sigma-Aldrich (St. Louis, MO). Toray carbon paper (TP) TGPH-060, was obtained from E-TEK, New Jersey, US (now a division of BASF). All other reagents and chemicals were of analytical grade and obtained from standard commercial sources. Enzyme stock solutions were prepared in sodium acetate buffer (0.5 M, pH 6.5) and $AuCl_4^-$ dilutions were prepared in distilled water. Glucose solutions were prepared from a pure substrate, dissolved in distilled water and equilibrated at room temperature before the experiments for mutarotation.

2.2. Preparation of the Glucose Oxidase – Gold Composites

GOx-Au composite particles were prepared as follows: 20 μL of GOx (300 mg/mL) was added to 175 μL of sodium acetate buffer (0.5 M, pH 6.5). To this was added a 5 μL aliquot of $AuCl_4^-$ at five dilutions: 30%, 15%, 7.5%, 3.75% and 0% to give a final concentration of 35, 18, 9, 4 and 0 mM respectively (i.e. GOx-Au:35). The reaction mixture was incubated at room temperature in the light for 5 hours.

2.3. Preparation of Carbon Paper Electrodes

Carbon paper (TP) was cut into 4.5 mm diameter disks, washed in ethanol and rinsed with water. The TP disk was placed on top of a microcentrifuge filter with a 30 kDa molecular weight cutoff membrane (Ultrafree, Sigma-Aldrich, St. Louis, MO). 100 μL of the GOx-Au composite was placed on top of the TP and passed through the column by centrifugation ($5585 \times g$). The molecular weight cut off membrane slows the passage of the gold particles to aid in entrapment. A control electrode with GOx alone was prepared in the same manner to allow for measurement of GOx activity that is retained by simple molecular weight size exclusion and physical adsorption. The TP modified GOx-Au electrodes were removed and washed with distilled water before analysis.

2.4. Characterization of Glucose Oxidase – Gold Composites

The spectroscopic characteristics of GOx-Au nanoparticles were measured using a Nanodrop 1000 (Thermo Fisher Scientific, Waltham, MA). The surface morphology of the GOx-Au electrodes were visualized using an Hitachi (S-2600) scanning electron micrscope (SEM) operating under vacuum at 20 kV for imaging. No conductive coatings were added to the sample electrodes prior to SEM analysis. Particle size was measured by dynamic light scattering using a Zetasizer nano CZ90 (Malvern Instruments Ltd., Worchestershire, UK) using a refractive index of 0.47 for gold [27]. Reported particle size measurements are an average of three samples (>12 measurements per sample). Attenuated Total Reflectance Fourier Transform-Infrared Spectroscopy (ATR FT-IR) was performed using a Nicolet FT-IR 6700 spectrophotometer equipped with a Smart Miracle single bounce diamond ATR accessory (Thermo Fisher Scientific, Waltham, MA). The data collection was completed using OMNIC 2.1 software. For FT-IR, 5 μL of GOx-Au composites were deposited onto a glass cover slip and allowed to dry. The cover slip was placed face down on the diamond surface of the FT-IR for analysis.

2.5. Treatment and Modification of Commercial Enzyme Preparations

In order to confirm the involvement of GOx in gold reduction, soluble contaminants were removed from the commercial enzyme preparation by dialysis. GOx (10 mL of 300 mg/mL) was dialyzed against three changes of 1 L sodium acetate buffer (0.5 M, pH 6.5) over 24 hours using a 10 kDa molecular weight cut off dialysis cassette (Slide-a-lyser; Pierce Inc., Rockford, IL).

The modification of the free cysteine thiol groups of GOx was adopted from a method reported previously [25]. A stock solution of 6 mM 2,2′-dithiobis(5-nitro-pyridine) [DTNP] was prepared in DMSO and mixed with GOx in potassium phosphate buffer (20 mM, pH 7.0) to give a final concentration of 0.2 mL DTNP in 5 mL of buffer containing 15 mg GOx. A control of GOx was prepared in the same manner with DMSO alone. The reaction mixture was incubated at 4 °C overnight with stirring. The GOx was

 © 2010 Wiley-VCH Verlag GmbH & Co. KGaA, Weinheim

concentrated using an Amicon Ultra filter unit with a 30 kDa molecular weight cut off (Sigma-Aldrich, St.Louis, MO). The final protein concentration of the thiol-modifed and untreated GOx was determined by bicinchoninic acid (BCA) assay according to the manufacturers instructions (Pierce, Rockford, IL). The GOx concentration was normalized and used in the gold reduction reaction as described above.

2.6. Electrochemical Measurements

Electrochemical measurements were performed with a potentiostat (Princeton Applied Research, Model Versastat 3, Oak Ridge, TN) in a three-electrode cell consisting of the TP GOx-Au working electrode, a glassy carbon counter electrode (Metrohm, Switzerland) and an Ag/AgCl reference electrode (CH Instruments Inc., Austin, TX) in a 50 mL working volume. The electrolyte solution used throughout consisted of a 1:1 mixture of phosphate buffer (20 mM, pH 7.0) and KCl (0.1 M). Electrochemical experiments were carried out at room temperature. Cyclic voltammograms were used to calculate the electron transfer rate constant using the method of Laviron [28, 29]. Each GOx-Au/TP disk was placed into a modified teflon cap designed to fit snuggly onto a commerical glassy carbon disk electrode. The cell was sparged with nitrogen for 20 min before starting potentiostat measurements. Initial analysis was performed after subjecting the electrode to 10 cycles with potential from -0.8 to -0.2 V at a constant scan rate (20 mV/s). The electrodes were then analyzed with varied scan rate of 5, 10, 20, 40, 60, 80, 100, 200 and 500 mV/s for 1 cycle each. The cell was then sparged with oxygen for 1 hour and the cyclic voltammetry repeated from -0.8 to -0.2 V at a scan rate of 20 mV/s for 5 cycles. 25 mM glucose (filter sterilized) was added and the cell was sparged with oxygen for a further 5 minutes to aid mixing and then the CV cycles repeated. Peak maxima, heights and currents were determined from voltammograms using the V3 studio software (Princeton Applied Research).

3. Results and Discussion

3.1. Synthesis and Characterization of Glucose Oxidase – Gold Composites

Simple mixing of $AuCl_4^-$ in a buffered solution of GOx at ambient conditions resulted in a significant color change over 5 hours of incubation. The color transition is indicative of a change in the metal oxidation state from Au^{3+} to Au^0. No gold formation was observed after a period of 7 days with buffer and $AuCl_4^-$ alone, confirming that GOx is essential for gold reduction. UV-visible spectroscopy of the resulting precipitates shows the appearance of an absorption band at 540 – 570 nm, characteristic of the surface plasmon resonance for gold nanoparticles (Fig. 1). Glucose oxidase – gold (GOx-Au) composites were prepared at a range of molar concentrations that produced a shift in the absorption wavelength (and respective color of the reaction product) that is directly dependent upon the ratio of enzyme to $AuCl_4^-$ and is characteristic of a variation in gold nanoparticle size

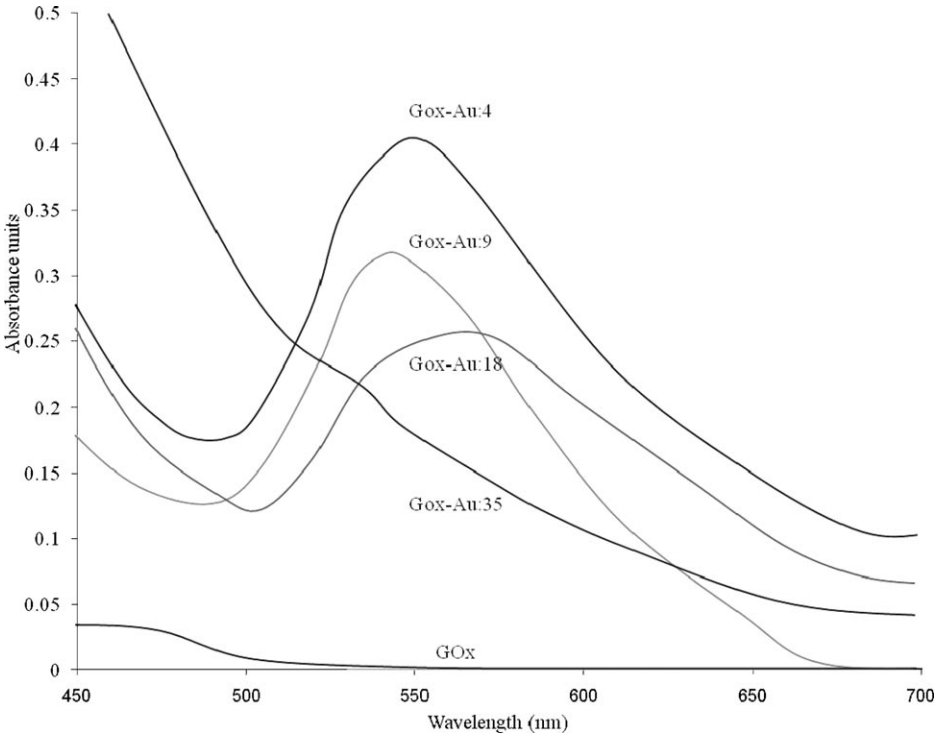

Fig. 1. UV/Vis absorption spectra of GOx-Au composites.

 © 2010 Wiley-VCH Verlag GmbH & Co. KGaA, Weinheim

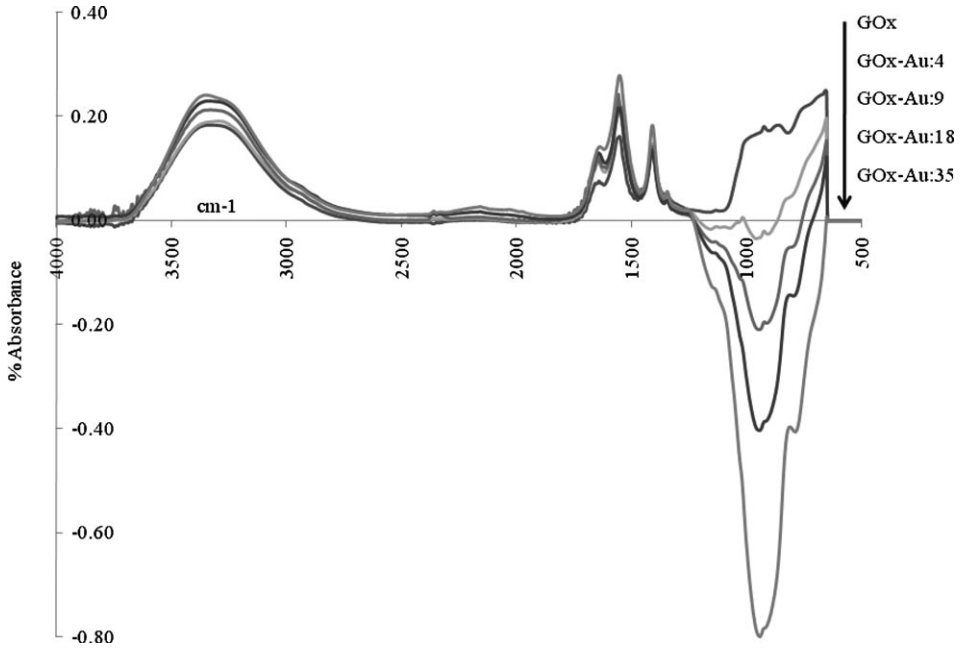

Fig. 2. FT-IR spectra of GOx-Au composites.

[16]. At high concentrations of $AuCl_4^-$ (GOx-Au:35), the formation of macromolecular gold particles is visible by eye. With decreasing concentration of $AuCl_4^-$, the product color changes through the visible range from yellow to orange (GOx-Au:18), brown (GOx-Au:9) and purple (GOx-Au:4).

FT-IR analysis of the GOx-Au composites showed uniform bond stretching characteristic of the native enzyme, irrespective of the gold particle size (Fig. 2). The amide bonds; amide-I, amide-II and amide-III of GOx are visible at 1630–1670 cm^{-1}, 1550 cm^{-1} and ca. 1340 cm^{-1} respectively [30]. A broad band attributed to NH stretch was also observed, centered around 3300 cm^{-1}. The results are in agreement with previous literature reports showing protein-mediated formation of gold particles [25]. The bond stretching associated with the native protein is retained within the GOx-Au composites indicating the retention of GOx within the gold particles with no apparent change in protein conformation. A broad band from 930–960 cm^{-1} was observed that increased relative to the apparent gold concentration and was absent with GOx alone.

Dynamic light scatter measurements revealed detail in the size distribution of nanoparticles in the GOx-Au composite materials that could not be ascertained from color and UV-visible spectroscopy observations (Table 1). The particle size distribution of GOx-Au:35 was polydisperse and indicated the presence of gold particle aggregates within the sample. The large aggregates scatter a significant portion of light due to their size but are present in low numbers. Lower concentrations of $AuCl_4^-$ in the reaction mixture resulted in homogeneous particle size distributions in terms of intensity and volume size distribution. GOx-Au:18 and GOx-Au:9 formed similarly sized gold particles in the order of 250–300 nm. The observed reduction of Au^{3+} to Au^0 suggests that GOx acts as a reducing agent for the metal and undergoes subsequent aggregation to form a planar microstructure. Gold synthesis in this way is therefore versatile as the size and morphology of the gold composites can be controlled by changing the ratio of $AuCl_4^-$ to GOx.

The material characterization using scanning electron microscopy (SEM) revealed a mixture of spheroid nanoparticles along with macromolecular gold triangles and platelets depending upon the gold precursor concentration of the preparation (Fig. 3). The TP fibers are clearly distinguishable by SEM. A well integrated coating of gold particles is visible for the GOx-Au:18 composite whereas larger macromolecular platelets were found in the GOx-Au:35 composite and tended to collect on the TP surface due to size restriction (Fig. 3). The formation of triangular and hexagonal particles at high gold concentrations is in agreement with previous reports that used biomolecules as templates for gold formation [22, 31].

Table 1. Stoichiometry and particle size distribution of GOx-Au composites.

Sample	Ratio Gox:Au [a]	Particle size	
		Intensity (nm)	Volume (nm)
GOx-Au:35	187:1	318.8 (85.8%) 71.4 (11.6%) 5483.0 (2.9%)	1040
GOx-Au:18	93:1	297.5	304.7
GOx-Au:9	47:1	255.0	252.6
GOx-Au:4	23:1	132.2	115.5

[a] Final concentration of GOx and Au assuming 100% incorporation

 © 2010 Wiley-VCH Verlag GmbH & Co. KGaA, Weinheim

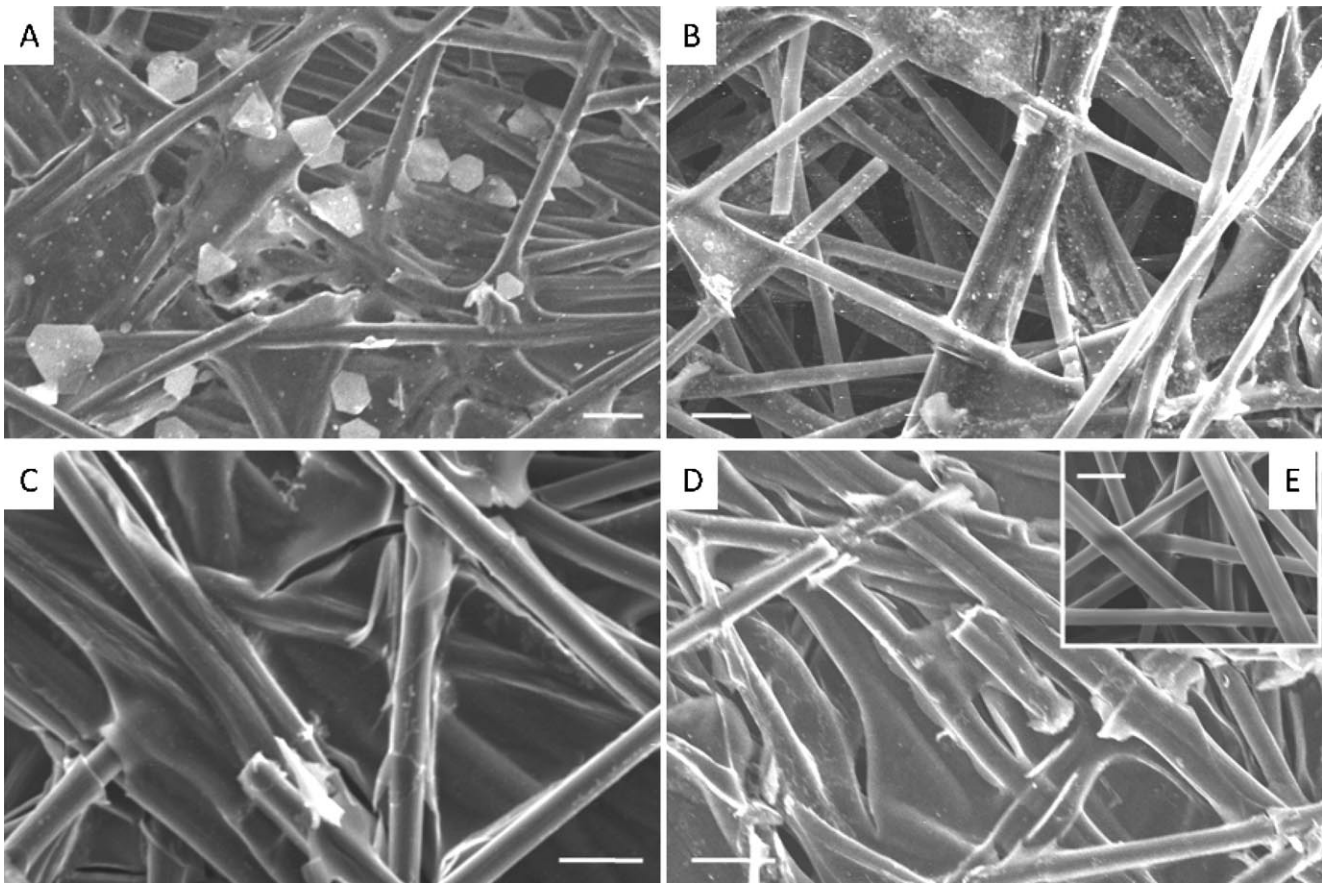

Fig. 3. Scanning electron micrographs of GOx-Au electrodes on carbon paper (TP). A) GOx-Au:35, B) GOx-Au:18, C) GOx-Au:9, D) GOx-Au:4, E) GOx. Scale bar = 20 μm

3.2. Direct Electrochemistry of Glucose Oxidase – Gold Composites

The electrochemical characteristics of the GOx-Au/TP electrodes were investigated by cyclic voltammetry (CV) in the presence and absence of oxygen (Fig. 4). GOx-Au:18 and GOx-Au:9 electrodes show reversible electron transfer and a pair of well-defined redox peaks with a formal redox potential of ca. −0.44 V (at pH 7.0 vs. Ag/AgCl) (Table 2). The standard redox potential of the FAD/$FADH_2$ redox couple at pH 7.0 is −0.43 V vs. Ag/AgCl [7]. The redox peaks are therefore attributed to the reversible reduction and oxidation reaction of the FAD/$FADH_2$ cofactor in the active site of GOx. Control experiments of TP with GOx alone (in the absence of gold nanoparticles) showed no discernible redox characteristics confirming that the gold particles provide the sole electrical connection between the enzyme and the electrode surface.

The theoretical half-height peak width for a one electron-transfer process is 91 mV at 298 K [32]. The redox peak separation (ΔE_p) and theoretical half peak heights measured for the GOx-Au:18 and GOx-Au:9 electrodes showed closest match to theoretical values for the electrodes tested (Table 2). The experimental peak width for GOx-Au:18 and GOx-Au:9 indicated that the FAD redox center of GOx shows a quasi-reversible one-electron transfer process on gold nanoparticles (Table 2). At the highest (GOx-Au:35) and lowest (GOx-Au:4) gold concentrations investigated, the peak width increases 3–5 fold. GOx-Au:35 and GOx-Au:4 electrodes show more variability and less stability in their redox characteristics, which may be attributed to the gold particle size. For example, large particle aggregates are retained on the electrode surface due to size exclusion, but may not connect well with the TP interface, whereas very small particles will likely pass straight through the TP carbon fiber matrix.

The ability of the gold encapsulated GOx to undergo DET with the electrode surface and retain its biocatalytic activity was investigated using cyclic voltammetry of solutions containing and lacking the substrates of the enzymatic recation: D-glucose and di-oxygen (Fig. 4). The oxidation of D-glucose by GOx involves a redox change of the FAD cofactor of the enzyme. Glucose is catalytically converted to gluconolactone with the concomitant conversion of oxygen to hydrogen peroxide. In the oxygenated electrochemical cell, the addition of glucose causes a decrease in current due to the catalytic removal of oxygen at the electrode surface. The addition of glucose to the GOx-Au electrodes in all

 © 2010 Wiley-VCH Verlag GmbH & Co. KGaA, Weinheim

Table 2. Direct electrochemistry characteristics of GOx-Au composites.
Scan rate 20 mV/s under a N_2 atmosphere with 25 mM glucose vs. Ag/AgCl; ND: not determined – not measurable at 20 mV/s scan rate.

Sample	Anodic peak		Cathodic peak		Formal potential (V)	ΔE_p (mV)	Half-height peak width (mV)
	(V)	(μA)	(V)	(μA)			
GOx-Au : 35	−0.417	1.38	−0.548	−3.47	−0.482	131	71 – 72
GOx-Au : 18	−0.435	4.02	−0.460	−5.30	−0.447	25	82 – 93
GOx-Au : 9	−0.420	2.30	−0.460	−3.14	−0.440	40	92 – 95
GOx-Au : 4	−0.392	1.33	−0.507	−2.77	−0.449	115	ND

cases resulted in a decrease in current density but to varying degrees. The current response confirmed the encapsulation of active GOx within the gold composites and is consistent with influence from enzyme that is in an intimate association with the electrode. The bioelectrocatalytic activity was greatest for GOx-Au : 18 and is again attributed to the gold particle size which allows for effective communication with the electrode.

3.3. Characterization of Bioelectrocatalytic Activity of Glucose Oxidase – Gold Composite Electrodes

From preliminary studies, the composition corresponding to the synthesis parameters of GOx-Au : 18 composites exhibited optimal direct electrochemical activity. Evidence of surface-confined redox centers was obtained from the observation of a correlation of anodic and cathodic peak

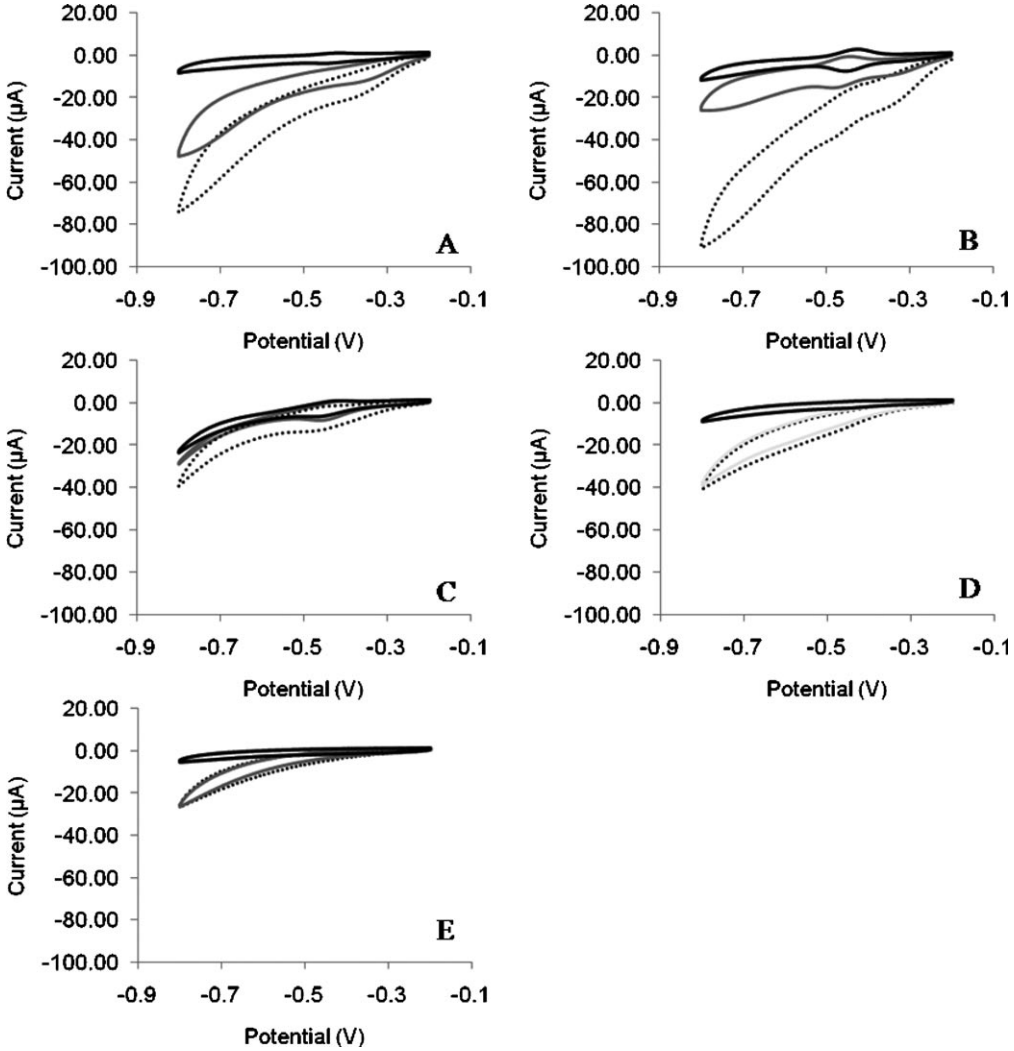

Fig. 4. Electrochemical analysis of GOx-Au electrodes: A) GOx-Au : 35, B) GOx-Au : 18, C) GOx-Au : 9, D) GOx-Au : 4, E) GOx on TP electrodes. Scan rate; 20 mV/s in 20 mM phosphate buffer/0.1 M KCl, (pH 7.0). N_2 saturated electrolyte (black line, #10 of 10 scans), O_2 saturated electrolyte +25 mM glucose (grey line, #5 of 5 scans), O_2 saturated electrolyte (dashed line, #5 of 5 scans).

 © 2010 Wiley-VCH Verlag GmbH & Co. KGaA, Weinheim

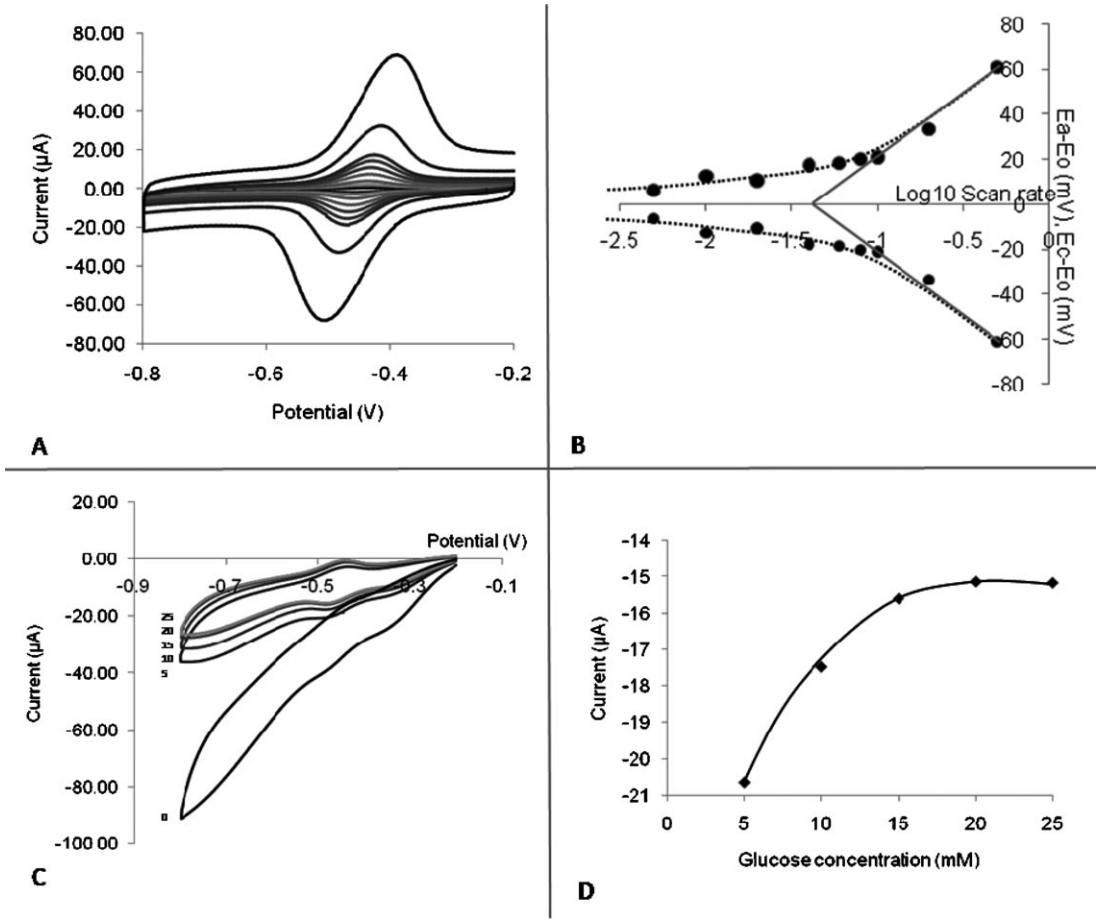

Fig. 5. Electrochemical analysis of GOx-Au:18 electrode. A) Effect of increasing scan rate from 5 to 500 mV/s (from inner scan outwards) in 20 mM phosphate buffer / 0.1 M KCl (pH7.0) and the corresponding Laviron plot (B). Effect of glucose concentration on current; cyclic voltammetry at 0, 5, 10, 15, 20 and 25 mM glucose (C) and the corresponding calibration curve (D).

currents against scan rate (Fig. 5A). The peak separation from 10 to 100 mV/s for electrode GOx-Au:18 ranges from 27.64 ($\pm$3.08) minimum to 45.08 ($\pm$4.36) maximum, indicating that the electron-transfer process is rapid and reversible. The separation between reduction and oxidation peak maxima as a function of scan rate was used to calculate an electron transfer rate (K_s) of 2.59 s^{-1} ($n=3$) for a triplicate of GOx-Au:18 electrodes [28]. The fast electron transfer indicates that the gold matrix provides an effective electrical communication between the FAD redox center and the TP electrode. The symmetry evident in the Laviron plot is indicative of a quazi-reversible charge-transfer process associated with the redox couple FAD/$FADH_2$ in the active site of the enzyme (Fig. 5B). In instances where the protein (GOx) is denatured, the cathodic peak positions shift more significantly than the anodic ones, resulting in asymmetrical Laviron plots. This allows us to hypothesize that, the voltammetry observations of redox activity at cathodic potentials are not a product of FAD cofactor that may have been released from the enzyme during denaturation and subsequently bound to the electrode composite matrix.

The CV of GOx-Au:18 undergoes a significant change in current density in the presence of oxygen attributed to the catalytic conversion of O_2 to H_2O_2 (Fig. 5C). It is confirmed that in oxygen-saturated buffer, the addition of glucose causes a decrease in current due to catalytic removal of oxygen at the electrode surface, confirming an intimate association between GOx and the gold composite. The bioelectrooxidation of glucose by the GOx-Au:18/TP electrode increases with glucose concentration up to a value of 15 mM at which point the kinetics of catalytic activity plateau as expected as a result of enzymatic Michaelis-Menten kinetics (Fig. 5D). Interestingly, the linear detection range for this system covers the physiological level of ca. 4–6 mM present in human blood, lending itself to a potential application in reagentless glucose detection.

3.4. Catalytic Mechanism of Glucose Oxidase – Gold Composites

Although a complete understanding of the mechanism for biocatalytic gold reduction remains unclear, it is generally believed that the nature of the amino acid functional groups

 © 2010 Wiley-VCH Verlag GmbH & Co. KGaA, Weinheim

(−SH, $-NH_2$, etc.) play an important role in gold reduction and aggregation. As stabilizing agents in gold nanoparticles synthesis, the most common groups are alkanethiols [25, 33]. The thiol-gold bond is most commonly described as a surface bound thiolate [33]. Recently, the presence of free thiol groups has been proposed as a mechanism for gold reduction in pure enzymes [25]. The thiol group (−SH) in the side chain of cysteine residues are known to react with gold to form Au-S bonds and is implicated as a mechanism for gold reduction in α-amylase and other enzymes with exposed thiol groups [25]. Similarly, glutathione reductase catalyzes the NADPH-dependent reduction of $AuCl_4^-$ to form gold nanoparticles via catalytic cysteines within the enzyme active site [34]. The involvement of disulfide bridges in gold reduction by bovine serum albumin has recently been proposed, although the purity (and potential presence of contaminants) of the commercial protein preparation was not reported [22]. Recent studies also propose an alternative mechanism in which aromatic amines can be used as reducing and capping agents for the synthesis of gold nanoparticles [35–38]. Selvakannan et al., for example, reported a water-soluble gold nanoparticle, functionalized with the amino acid lysine [39]. Similarly, Subramaniam et al. stated that the reduction of auric ions and the oxidation of the aromatic amine occur simultaneously [38]. The oxidative polymerization of the amines proceeds simultaneously with the formation of gold nanoparticles such that the polymerized amine encapsulates the gold nanoparticle. As such, the interaction of the amines with gold is strong and similar to thiolate bonds [37]. GOx contains two disulfide bridges and two free sulfhydryl groups as well as amino groups presented on the surface [40]. GOx possesses thirteen lysine residues on its surface and as a result, carries a net negative charge. The thiol group (−SH) in the side chain of cysteine residues and amine groups of GOx may therefore be proposed to be responsible for the synthesis of gold nanoparticles.

Additional experiments were pursued to examine the GOx-catalyzed gold reduction in light of other literature reports. After GOx was dialyzed against acetate buffer to limit potential contaminants from the commercial preparation, the gold reduction activity was retained in the dialyzed GOx, confirming that GOx is indeed the active component within the mixture. The rate of gold reduction was higher, however, in the crude commercial preparation suggesting that a component in the mixture may accelerate gold particle formation (Fig. 6). We must emphasize, however, that no seed particles, additional glucose or exogenous reaction components were added to the commercial GOx preparation during gold reduction. Results from preliminary experiments in which GOx was treated with DTNP to modify the free thiol groups [25], remained inconclusive, as the reaction was complicated by the requirement for DMSO in the reaction mixture. A more detailed investigation of the kinetics and reaction mechanism of gold reduction from highly purified GOx is therefore currently underway.

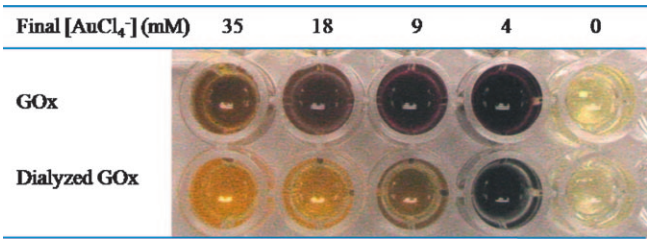

Fig. 6. Formation of GOx-Au composites from crude and dialyzed GOx (48 hours incubation).

4. Conclusions

The method describes a simple and benign method to associate GOx in metallic gold nanoparticles via GOx-catalyzed gold reduction. The gold particles form in such a way that they facilitate electron transfer between the redox center of GOx and an electrode surface. The electron transfer system requires no external mediator and the effective communication of electrons between GOx and the electrode occurs at a potential of approximately −0.44 V. Such a negative potential provides an effective anode configuration for enzyme-based fuel cell applications or efficient interference-free biosensing electrodes. The GOx-Au composites demonstrate an electron transfer rate comparable to immobilization utilizing carbon nanotubes but with the advantage of simplicity of preparation that potentially may result in higher technology adaptability and better manufacturability and technology development. The bio-conjugates of GOx-Au form nanoparticles under benign physiological conditions in an aqueous solvent and the reaction can be tuned to control size and shape of metal nanoparticles with varied optical properties.

Acknowledgements

The UNM portion of this work was supported in part by a grant from DOD/AFOSR MURI Award Number: FA9550-06-1-0264, Fundamentals and Bioengineering of Enzymatic Fuel Cells. AFRL research was funded by the US Air Force Research Laboratory, Materials Science Directorate and the Air Force Office of Scientific Research.

References

[1] A. Kaminska, O. Inya-Agha, R. J. Forster, T. E. Keyes, *PhysChemChemPhys* **2008**, *10*, 4172.
[2] S. Liu, D. Leech, H. Ju, *Anal. Lett.* **2003**, *36*, 1.
[3] J. M. Pingarron, P. Yanez-Sedeno, A. Conzalez-Cortes, *Electrochim. Acta* **2008**, *53*, 5848.
[4] I. Willner, B. Basnar, B. Willner, *FEBS J.* **2007**, *274*, 302.
[5] R. Baron, B. Willner, I. Willner, *Chem. Commun.* **2007**, 323.
[6] Y. Xiao, F. Patolsky, E. Katz, J. F. Hainfield, I. Willner, *Science* **2003**, *299*, 1877.
[7] A. Guiseppi-Elie, C. Lei, R. H. Baughman, *Nanotechnology* **2002**, *13*, 559.

 © 2010 Wiley-VCH Verlag GmbH & Co. KGaA, Weinheim

[8] J. Zhang, M. Feng, H. Tachikawa, *Biosens. Bioelectron.* **2007**, *22*, 3036.
[9] H. J. Hecht, H. M. Kalisz, J. Hendle, R. D. Schmid, D. Schomburg, *J. Mol. Biol.* **1993**, *229*, 153.
[10] B. Willner, E. Katz, I. Willner, *Curr. Opin. Biotechnol.* **2006**, *17*, 589.
[11] D. Ivnitski, K. Artyushkova, R. A. Rincon, P. Atanassov, H. R. Luckarift, G. R. Johnson, *Small* **2008**, *4*, 357.
[12] D. Ivnitski, B. Branch, P. Atanassov, C. Apblett, *Electrochem. Commun.* **2006**, *8*, 1204.
[13] Y.-M. Yan, R. Tel-Vered, O. Yehezkeli, Z. Cheglakov, I. Willner, *Adv. Mater.* **2008**, *20*, 2365.
[14] S. Zhao, K. Zhang, Y. Bai, W. Yang, C. Sun, *Bioelectrochemistry* **2006**, *69*, 158.
[15] A. Heller, *Nat. Biotechnol.* **2003**, *21*, 631.
[16] M. C. Daniel, D. Astruc, *Chem. Rev.* **2004**, *104*, 293.
[17] A. Bharde, A. Kulkarni, M. Rao, A. Prabhune, M. Sastry, *J. Nanosci. Nanotechnol.* **2007**, *7*, 4369.
[18] M. I. Husseiny, M. A. El-Aziz, Y. Badr, M. A. Mahmoud, *Spectrochim. Acta* **2007**, *67*, 1003.
[19] P. Mukherjee, S. Senapati, D. Mandal, A. Ahmad, M. I. Khan, R. Kumar, M. Sastry, *ChemBioChem* **2002**, *3*, 461.
[20] G. Singaravelu, J. S. Arockiamary, V. G. Kumar, K. Govindaraju, *Coll. Surf.* **2007**, *57*, 97.
[21] J. M. Slocik, M. O. Stone, R. R. Naik, *Small* **2005**, *1*, 1048.
[22] N. Basu, R. Bhattacharya, P. Mukherjee, *Biomed. Mater.* **2008**, *3*, 034105.
[23] R. Ben-Knaz, D. Avnir, *Biomaterials* **2009**, *30*, 11263.
[24] A. Gole, C. Dash, C. Soman, S. R. Sainkar, M. Rao, M. Sastry, *Bioconj. Chem.* **2001**, *12*, 684.
[25] A. Rangnekar, T. K. Sarma, A. K. Singh, J. Deka, A. Ramesh, A. Chattopadhyay, *Langmuir* **2007**, *23*, 5700.
[26] I. Willner, R. Baron, B. Willner, *Adv. Mater.* **2006**, *18*, 1109.
[27] G. Charter, Index of Refraction; in *Introduction to Optics*, Springer, New York **2005**, p. 351.
[28] E. Laviron, *J. Electrochem. Anal.* **1979**, *101*, 19.
[29] P. Atanasov, V. A. Bogdanovskaja, I. Iliev, M. R. Tarasevich, V. Vorob'ev, *Soviet Electrochem.* **1989**, *25*, 1320.
[30] A. Haouz, C. Twist, C. Zentz, P. Tauc, B. Alpert, *Eur. Biophys. J.* **1998**, *27*, 19.
[31] S. Shiv Shankar, A. Rai, B. Ankamwar, A. Singh, A. Ahmad, M. Sastry, *Nat. Mater.* **2004**, *3*, 482.
[32] A. J. Bard, L. R. Faulkner, *Electrochemical Methods; Fundamentals and Applications*, Wiley, New York **1980**, p. 718.
[33] M. Hasan, D. Bethell, M. Brust, *J. Am. Chem. Soc.* **2002**, *124*, 1132.
[34] D. Scott, M. Toney, M. Muzikar, *J. Am. Chem. Soc.* **2008**, *130*, 865.
[35] C. C. Chen, C. H. Hsu, P. L. Kuo, *Langmuir* **2007**, *23*, 6801.
[36] Y. Ding, X. Zhang, X. Liu, R. Guo, *Langmuir* **2006**, *22*, 2292.
[37] A. Kumar, S. Mandal, P. R. Selvakannan, R. Pasricha, A. B. Madale, M. Sastry, *Langmuir* **2003**, *19*, 6277.
[38] C. Subramaniam, R. T. Tom, T. Pradeep, *J. Nanoparticle Res.* **2005**, *7*, 209.
[39] P. R. Selvakannan, S. Mandal, S. Phadtare, R. Pasricha, M. Sastry, *Langmuir* **2003**, *19*, 3545.
[40] R. Wilson, A. P. F. Turner, *Biosens. Bioelectron.* **1992**, *7*, 165.

 © 2010 Wiley-VCH Verlag GmbH & Co. KGaA, Weinheim